Time integrated search for point sources of cosmic neutrinos with the ANTARES telescope

Claudio Bogazzi on behalf of the ANTARES Collaboration

claudiob@nikhef.nl, NIKHEF institute, Science Park 105, 1098 XG, Amsterdam, The Netherlands

Abstract

Results of a time-integrated search for astrophysical high-energy neutrinos are presented using data collected from January 2007 to December 2010 with the ANTARES neutrino telescope. An unbinned likelihood ratio method is used to search for signal events. The final sample consists of 3058 events. Simulations estimate 84% to be neutrinos, while the rest are mis-reconstructed atmospheric muons. A full sky survey as well as a search on a pre-defined list of candidate objects was performed. No evidence for a signal is found and neutrino flux upper limits have been obtained. The neutrino flux sensitivity is $2.6 \times 10^{-8}(\mathrm{E/GeV})^{-2}\mathrm{GeV}^{-1}\mathrm{s}^{-1}\mathrm{cm}^{-2}$ for the part of the sky that is always visible (declination $\leq$ -48 degrees) which corresponds to almost a factor 3 better than the previous search.

Keywords: ANTARES, point source search

1. Introduction

The origin of high-energy Cosmic Rays (CRs) as well as their acceleration mechanism is still unknown. Supernova remnants, microquasars and active galactic nuclei are just few examples of possible acceleration sites that have been suggested in the past [1]. Neutrinos, being neutral and weakly interacting, can travel long distances without being absorbed or deflected and therefore they can be the key to understand the origin of CRs.

1.1. The ANTARES detector

The ANTARES detector, located at a depth of 2475 m in the Mediterranean Sea, 42 km from Toulon in France (42°48 N, 6°10 E), consists of a tri-dimensional array of 885 photomultipliers (PMTs) arranged on 12 vertical lines. Each PMT is housed in a pressure resistant glass sphere called Optical Module (OM). The OMs are grouped in 25 triplets, called storeys, per line. The spacing between storeys is 14.5 m while the lines are separated by 60-70 m and kept vertical by a buoy.

The telescope operates by detecting Cherenkov light induced by relativistic muons that result from neutrino interactions in or around the detector. The arrival time and amplitude of the Cherenkov light on the PMTs are digitized into 'hits' [2] and transmitted to shore where they are used to reconstruct the muon trajectory.

2. Data sample

This analysis is based on data collected between January 31st 2007 and December 30th 2010. During these four years, the detector consist of 5 lines for most of 2007 and of 9, 10 and 12 lines for the remaining years. The total integrated livetime is 813 days.

Muon tracks are reconstructed from the hits using an algorithm based on a maximum likelihood method [3]. A multi-stage fitting procedure guarantees the maximization of the likelihood of the observed hit times as a function of the muon direction and position. The goodness of the fit is measured by the reconstruction variable $\Lambda = \log(L)/N_{\mathrm{dof}} + 0.1 \times (N_{\mathrm{comp}} - 1)$ with $\log(L)/N_{\mathrm{dof}}$ the reduced log-likelihood per degree of freedom and N_{comp} the number of times the fitting procedure converged to the same result ($N_{\mathrm{comp}} = 1$ for the majority of the badly reconstructed events, while it can be as large as 9 for well reconstructed events [3]). The cumulative distribution of Λ for upward-going events is shown in Figure 1 with the simulated contributions of atmospheric muons and neutrinos. Atmospheric muons are simulated with the MUPAGE package [4]; neutrinos are instead generated with the GENNEU [5] package with the flux from [6] based on a 1-dimensional calculation approach, i.e. all secondary particles in the shower are considered collinear with primary cosmic rays.

Upward-going neutrino candidate events are selected applying the following cuts:

- $\Lambda > -5.2$. This minimum value for the reconstruction quality variable Λ has been chosen in order to optimize the background rejection and the signal efficiency for the discovery potential.
- $\beta < 1°$. A second cut is applied on the angular uncertainty obtained from the likelihood fit β, i.e. the estimate of the error on the direction of the reconstructed muon track, in order to reject further

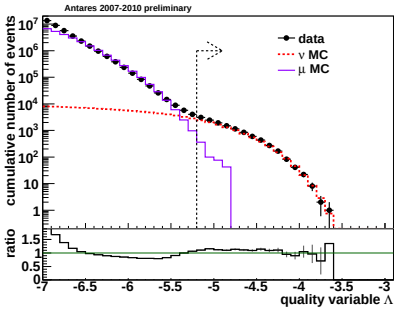

Figure 1 Cumulative distribution of the reconstructed quality variable Λ. The solid line is for simulated atmospheric muons while the dashed line corresponds to simulated atmospheric neutrinos. The bottom plot shows the ratio between data and Monte Carlo.

mis-reconstructed atmospheric muons.

The final sample consists of 3058 events. From simulation the mis-reconstructed atmospheric muon contribution is estimated to be 16%.

3. Detector performance

The two crucial parameters which describe the performance of a neutrino telescope are the angular resolution, i.e. the median angle between the neutrino and the reconstructed muon, and the acceptance. In the presented analysis both parameters are obtained from simulation.

3.1. Angular resolution

The cumulative distribution of the angle between the reconstructed muon track and the true neutrino direction is shown in Figure 2 for selected neutrino events assuming a spectrum proportional to E_ν^{-2} where E_ν is the neutrino energy. The median of this distribution is 0.46 ± 0.10 degrees. 83% of the selected events are reconstructed better than 1 degree.

The systematic uncertainty on the angular resolution has been computed by artificially deteriorating the simulated timing accuracy. This is done by smearing the hit times in the simulation according to a Gaussian with a width of σ_t. A comparison between the Λ distribution of the resulting simulation with the observed atmospheric neutrino events excludes a smearing of 3 ns which was found to be incompatible with data at the 2σ level where σ is the uncertainty on the flux model [7]. The best agreement between data and Monte Carlo is obtained with $\sigma_t = 2 \pm 0.5$ ns. Hence, this value is used as a standard value for the simulations presented in this work.

3.2. Acceptance

The acceptance of the detector is expressed in terms of the effective area, $A_\nu^{\rm eff}$ defined as the ratio between the selected neutrino event rate and the cosmic neutrino flux.

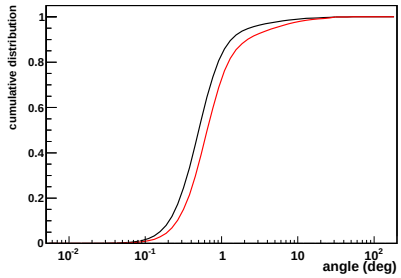

Figure 2 Cumulative distribution of the angle between the reconstructed muon track and the true neutrino track for selected signal events assuming a neutrino spectrum proportional to E_ν^{-2}. The red line is for the subset of data in which only 5 lines were operational. The black line shows the results for the total set of data used.

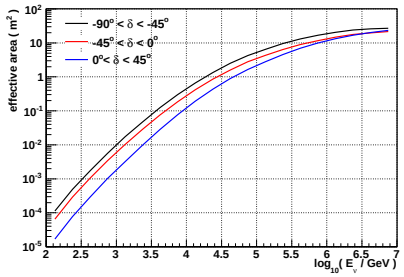

Figure 3 Neutrino effective area for the selected events as a function of the neutrino energy for three different declination bands.

Figure 3 shows the distribution of $A_\nu^{\rm eff}$ as a function of the neutrino energy for three different declination intervals for a sum of $\nu_\mu + \bar{\nu}_\mu$ fluxes, assumed to be equal.

To constrain the systematic uncertainty on the acceptance, a comparison between the atmospheric neutrino data and the simulation with a maximum of 15% reduction of the photon detection probability of the OMs has been made. Despite this reduction in the OMs efficiency, data and simulation are still compatible within the 30% systematic uncertainty on the neutrino flux [7]. Hence, a 15% systematic uncertainty on the acceptance is used in the limit computation.

4. Search method

The algorithm uses an unbinned maximum likelihood ratio defined as:

$$\log \mathcal{L}_{\rm s+b} = \sum_i \log[\mu_{\rm sig} \times \mathcal{F}(\beta_i(\delta_{\rm s}, \alpha_{\rm s})) \times \mathcal{N}^{\rm sig}(N^i_{\rm hits}) + \\ + \mathcal{B}(\delta_i) \times \mathcal{N}^{bg}(N^i_{\rm hits})] + \mu_{\rm sig}, \quad (1)$$

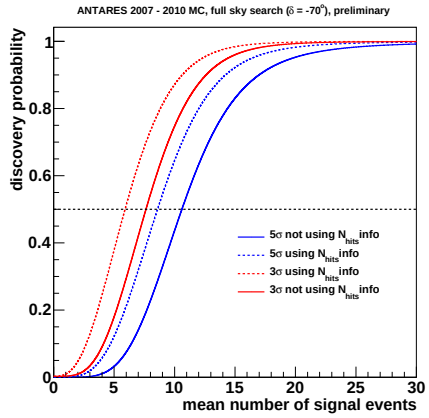

Figure 4 Probability for a 3σ(red lines) and 5σ (blue lines) full-sky search discovery as a function of the mean number of signal events from a source at $\delta = -70°$ with a neutrino spectrum proportional to E_ν^{-2}. The dotted lines are for the likelihood described, the solid lines refer to the case where $N_{\rm hits}$ was not used.

where the sum is over the events, $\mathcal{F}$ is a parametrization of the point spread function, i.e. the probability density function (pdf) of reconstructing event i at a distance β_i from the true source location $(\delta_{\rm s}, \alpha_{\rm s})$; $\mathcal{B}$ is a parametrization of the background rate obtained from the distribution of the observed declination of the selected events; μ_{sig} is the mean number of selected signal events; $N_{\rm hits}$ is the number of hits used in the reconstruction. $\mathcal{N}^{\rm sig}(N^i_{\rm hits})$ and $\mathcal{N}^{\rm bg}(N^i_{\rm hits})$ are the probabilities of measuring N_{hits} for signal and background respectively.

The test statistic is computed by fitting the likelihood. In case of a candidate list search, the only free parameter is the mean number of selected signal events $\mu_{\rm sig}$, while in the full-sky search a first selection of significant clusters is performed requiring at least four events in a cone of 3 degrees and then the likelihood is maximized by fitting besides $\mu_{\rm sig}$ also the source coordinates $(\delta_{\rm s}, \alpha_{\rm s})$.

Simulations show that by using the number of hits information in the likelihood the discovery potential improves by a factor 28% (21%) for the 3(5)σ discovery probability as shown in Figure 4.

5. Results

5.1. Full-sky search

The most significant deviation from background is located at $(\delta, \alpha) = (-46.5°, -65°)$. The fit assigns 5 events above the background within 1 degree with a value of the test statistic of $\mathcal{Q} = 13.1$ which corresponds to a p-value of 2.6%. Figure 5 shows a sky map of the selected events in galactic coordinates with the location of the most signal like cluster.

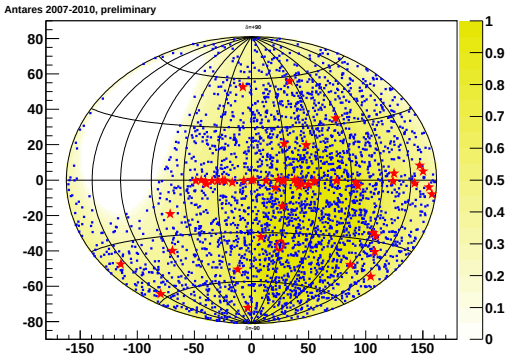

Figure 5 Galactic skymap showing the 3058 data events. The position of the most signal-like cluster is indicated by the circle. The stars denote the position of the 51 candidate sources.

5.2. Candidate list search

Table 1 shows the results of the search in the direction of 51 pre-defined candidate sources.

The most signal-like candidate source is HESS J1023-575 with a post-trial p-value of 41%.

Figure 6 shows the 90% CL limits on the neutrino flux assuming a neutrino spectrum proportional to E_ν^{-2} using the Feldman-Cousing prescription [9]. In the same Figure the sensitivity of this analysis which is a factor 2.7 better compared with the sensitivity obtained with 2007 and 2008 only data [8]. It is also relevant to highlight the difference in the sensitivity curves for ANTARES and IceCube. As can be seen in Figure 6 the sensitivity for IceCube coincides mostly with the best upper limits, i.e. the ones which are most background-like, while for ANTARES it corresponds exactly to the median of the upper limits (50% of the upper limits are above the sensitivity line, 50% are below). This different behaviour can be explained by the way in which the test statistic for the background-only case is derived and its response to background fluctuations.

6. Cross-check

All the results presented have been cross-checked by a second analysis which applies the Expectation-Maximisation (EM) method to the search of point sources [14], using the same data set.

The EM method is an iterative procedure to maximum likelihood estimation which consists of two steps: the expectation, where the log-likelihood is evaluated for a given set of initial parameters describing the (unknown) source properties, and the maximisation, where a new set of parameters which maximise the likelihood is found. For this study, these paramaters were the number of signal events, the source location and the standard deviations of a two-dimensional Gaussian which describes the signal pdf.

With this method, the most signal-like cluster in the full-sky search is still located at $(\delta, \alpha) = (-46.5°, -64.9°)$.

source	$\alpha_s(^\circ)$	$\delta_s(^\circ)$	p	$\phi^{90\%\mathrm{CL}}$
HESS J1023-575	155.83	-57.76	0.41	6.6
3C 279	-165.95	-5.79	0.48	0.1
GX 339-4	-104.30	-48.79	0.72	5.8
Cir X-1	-129.83	-57.17	0.79	5.8
MGRO J1908+06	-73.01	6.27	0.82	0.1
ESO 139-G12	-95.59	-59.94	0.94	5.4
HESS J1356-645	-151.00	-64.50	0.98	5.1
PKS 0548-322	87.67	-32.27	0.99	7.1
HESS J1837-069	-80.59	-6.95	0.99	8.0
PKS 0454-234	74.27	-23.43	1.00	7.0
IceCube hotspot	75.45	-18.15	1.00	7.0
PKS 1454-354	-135.64	-35.67	1.00	5.0
RGB J0152+017	28.17	1.79	1.00	6.3
Geminga	98.31	17.01	1.00	7.3
PSR B1259-63	-164.30	-63.83	1.00	3.0
PKS 2005-489	-57.63	-48.82	1.00	2.8
HESS J1616-508	-116.03	-50.97	1.00	2.7
HESS J1503-582	-133.54	-58.74	1.00	2.8
HESS J1632-478	-111.96	-47.82	1.00	2.6
H 2356-309	-0.22	-30.63	1.00	3.9
MSH 15-52	-131.47	-59.16	1.00	2.6
Galactic Center	-93.58	-29.01	1.00	3.8
HESS J1303-631	-164.23	-63.20	1.00	2.4
HESS J1834-087	-81.31	-8.76	1.00	4.3
PKS 1502+106	-133.90	10.52	1.00	5.2
SS 433	-72.04	4.98	1.00	4.6
HESS J1614-518	-116.42	-51.82	1.00	2.0
RX J1713.7-3946	-101.75	-39.75	1.00	2.7
3C454.3	-16.50	16.15	1.00	5.5
W28	-89.57	-23.34	1.00	3.4
HESS J0632+057	98.24	5.81	1.00	4.6
PKS 2155-304	-30.28	-30.22	1.00	2.7
HESS J1741-302	-94.75	-30.20	1.00	2.7
Centaurus A	-158.64	-43.02	1.00	2.1
RX J0852.0-4622	133.00	-46.37	1.00	1.5
1ES 1101-232	165.91	-23.49	1.00	2.8
Vela X	128.75	-45.60	1.00	1.5
W51C	-69.25	14.19	1.00	3.6
PKS 0426-380	67.17	-37.93	1.00	1.4
LS 5039	-83.44	-14.83	1.00	2.7
W44	-75.96	1.38	1.00	3.1
RCW 86	-139.32	-62.48	1.00	1.1
Crab	83.63	22.01	1.00	4.1
HESS J1507-622	-133.28	-62.34	1.00	1.1
1ES 0347-121	57.35	-11.99	1.00	1.9
VER J0648+152	102.20	15.27	1.00	2.8
PKS 0537-441	84.71	-44.08	1.00	1.3
HESS J1912+101	-71.79	10.15	1.00	2.5
PKS 0235+164	39.66	16.61	1.00	2.8
IC443	94.21	22.51	1.00	2.8

Table 1 Results of the candidate source search. The source coordinates and the p-values (p) are shown as well as the limits on the flux intensity $\phi^{90\%\mathrm{CL}}$ in units $10^{-8}\mathrm{GeV}^{-1}\mathrm{cm}^{-2}\mathrm{s}^{-1}$.

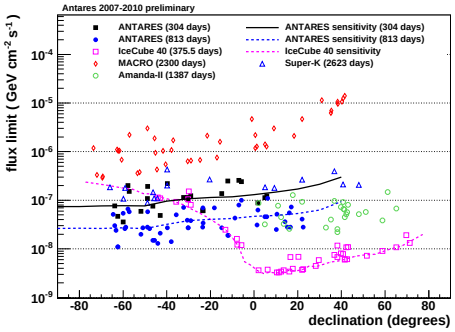

Figure 6 Limits set on the normalisation ϕ of an E_ν^{-2} spectrum of high-energy neutrinos from selected candidates (see Table 1). Also shown is the sensitivity, which is defined as the median expected limit. Several previously published limits on sources in both the Southern and Northern sky are also shown [8], [10], [11], [12], [13].

The number of signal events estimated by the algorithm is 5.3. The correspondig value of the test statistic is $\mathcal{Q} = 12.8$. None of the 51 candidate sources show an excess of signal events over the atmospheric neutrino background. The lowest p-value was found for the source 3C 279.

7. Conclusion

A time integrated search for high-energy cosmic neutrinos has been presented. Data were taken during the first four years of operation when ANTARES consist of 5 lines for most of the first year and 9, 10 and 12 for the rest. No statistically significant excess has been found for both the full-sky search and the candidate list search. Limits have been obtained on the neutrino flux. Most of them are up to now the most restrictive ones in the Southern sky.

References

[1] F. Halzen, D. Hooper, Rep. Prog. Phys., 2002, **65**, 1025
[2] J. A. Aguilar *et al.* , Nucl. Instr. Meth., 2010, **A622**, 59.
[3] A. Heijboer, 2004, PhD Thesis, http://antares.in2p3.fr/Publications.
[4] G. Carminati, M. Bazzotti, A. Margiotta and M. Spurio, Comp. Phys. Comm., **179**, 915.
[5] D. Bailey, 2002, PhD Thesis, http://antares.in2p3.fr/Publications.
[6] V. Agrawal, T. K. Gaisser, P. Lipari, T. Stanev Phys. Rev. D, 1996, **53**,1314.
[7] G. D. Barr *et al.* , Phys. Rev. D, 2006, **74**(9): 094009.
[8] S. Adrian-Martínez *et al.* (ANTARES Collaboration), ApJ, 2011, **743**, L14.
[9] G. J. Feldman and R. D. Cousins, Phys. Rev. D, 1998, **57**(7), 3873.
[10] M. Ambrosio *et al.* , ApJ, 2001, **546**, 1038.
[11] E. Thrane *et al.* , ApJ, 2009, **704**, 503.
[12] R. Abbasi *et al.* ,Phys. Rev. D., 2009, **79**, 062001.
[13] R. Abbasi *et al.* , ApJ, 2011, **732**: 18.
[14] J. A. Aguilar and J. J. Hernández-Rey, Astropart. Phys., 2008, **29**, 117.